Resistive state triggered by vortex entry in $YBa_2Cu_3O_{7-\delta}$ nanostructures

R.Arpaia[a,b], D.Golubev[c], R.Baghdadi[a], M.Arzeo[a], G.Kunakova[a,d], S.Charpentier[a], S.Nawaz[a], F.Lombardi[a], T.Bauch[a,*]

[a] *Quantum Device Physics Laboratory, Department of Microtechnology and Nanoscience, Chalmers University of Technology, SE-41296 Göteborg, Sweden*
[b] *CNR-SPIN, Dipartimento di Scienze Fisiche, Università degli Studi di Napoli Federico II, I-80126 Napoli, Italy*
[c] *Low Temperature Laboratory (OVLL), Aalto University School of Science, P.O. Box 13500, FI-00076 Aalto, Finland*
[d] *Institute of Chemical Physics, University of Latvia, LV-1586 Riga, Latvia*

Abstract

We have realized $YBa_2Cu_3O_{7-\delta}$ nanowires and nano Superconducting Quantum Interference Devices (nanoSQUID). The measured temperature dependence of the wire resistances below the superconducting transition temperature has been analyzed using a thermally activated vortex entry model valid for wires wider than the superconducting coherence length. The extracted zero temperature values of the London penetration depth, $\lambda_0 \simeq 270 \pm 15$ nm, are in good agreement with the value obtained from critical current modulations as a function of an externally applied magnetic field in a nanoSQUID implementing two nanowires.

Keywords: High-temperature superconductors, nanowires, nanoSQUIDs, phase slips, vortex dynamics

---

*Corresponding author
Email address: thilo.bauch@chalmers.se (T.Bauch)

The recent advances in nanopatterning techniques applied to type II superconductors allow to study the effect of single vortex dynamics on the electrical transport properties of superconducting nanowires. Indeed, there has been an increased interest in studying the transport properties of nanowires of thickness t smaller than the London penetration depth λ_L and of width w smaller than the Pearl length $\lambda_P = \lambda_L^2/t$ in the search for quantum tunneling of vortices [1, 2] and for the understanding of "dark-counts" in superconducting nanowire based single photon detectors [3]. In systems with reduced dimensionality it can also be observed that the superconducting phase transition is frequently not sharp and the measured dependence of the sample resistance $R(T)$ in the vicinity of T_C may have a finite width, even in absence of any sample inhomogeneity. This broadening is due to thermal fluctuations. In 1D wires ($w, t \ll \xi$) such fluctuations, called thermally activated phase slips (TAPS), with spatial extensions of the order of the coherence length ξ, hence extending throughout the wire cross-section, disrupt locally the flow of supercurrent, thereby imparting a non-zero resistance to the wire [4, 5, 6].

In the case of wide wires ($w \gg 4.44\xi$), vortex crossing from one edge of the bridge to the other, perpendicular to the bias current, has been found to be the dominant mechanism of dissipation [7, 8, 9]. In this paper we analyze the role of thermally activated vortex dynamics on dissipation close to the superconducting transition temperature T_C in nanowires made of the High critical Temperature Superconductor (HTS) $YBa_2Cu_3O_{7-\delta}$ (YBCO) and extract the zero temperature values λ_0 and ξ_0.

Following Ref. [9], and considering in addition the contribution of the vortex core energy [10, 11], the vortex entry potential formed by the supercurrents around the vortex center inside the wire and the Lorentz force induced by the bias current I_b in the case of homogeneous current flow ($w \ll \lambda_P$) is given as a function of the position y, parallel to the width, by:

$$\Delta U(y, I_b, T) = \mu^2 \epsilon_0(T) \left[\ln\left(\frac{2.94w}{\pi\xi} \sin\frac{\pi y}{w} \right) - \frac{I_b}{\mu^2 I_0(T)} \frac{\pi y}{w} \right] , \qquad (1)$$

with $I_0(T) = \Phi_0 t/4\mu_0\lambda_L^2(T)$ and $\epsilon_0(T) = \Phi_0^2 t/4\pi\mu_0\lambda_L^2(T)$ the characteristic energy of a vortex in thin films. Here $\Phi_0 = h/2e$ is the superconducting flux quantum and μ_0 is the vacuum permeability. The parameter μ^2 describes the order parameter suppression due to the bias current, which itself depends on the phase difference ϕ between the two ends of the wire:

$$\mu^2 = \frac{|\Psi|^2}{|\Psi_\infty|^2} = 1 - \left(\frac{\phi\xi}{l}\right)^2 . \qquad (2)$$

Here Ψ_∞ is the equilibrium order parameter in the absence of the external field and transport current and l is the wire length. The bias current at which the vortex entry barrier goes to zero and vortices can enter the superconducting wire is approximately given by the depairing critical current [9, 12, 13].

From the vortex crossing rate obtained in Ref. [9] in the framework of the Langevin equation for viscous vortex motion and invoking the known solution of the corresponding Fokker-Plank equation one can write for the zero bias resistance of a nanowire with length l:

$$R_v(T) = 7.1\, R_\square \frac{l\xi(T)}{w^2} \left(\frac{\epsilon_0(T)}{k_B T}\right)^{3/2} \exp\left(-\frac{\epsilon_0(T)}{k_B T} \ln\frac{1.47w}{\pi\xi(T)} \right) , \qquad (3)$$

where $R_\square$ is the sheet resistance of the wire, k_B is the Boltzmann constant, and considering that μ^2 is equal to 1 in the zero bias limit.

In this work we have patterned Au capped YBCO nanowires using e-beam lithography from YBCO films grown on MgO (110) and MgO (001) substrates (see Fig. 1(a)). Details of the nano-fabrication process have been

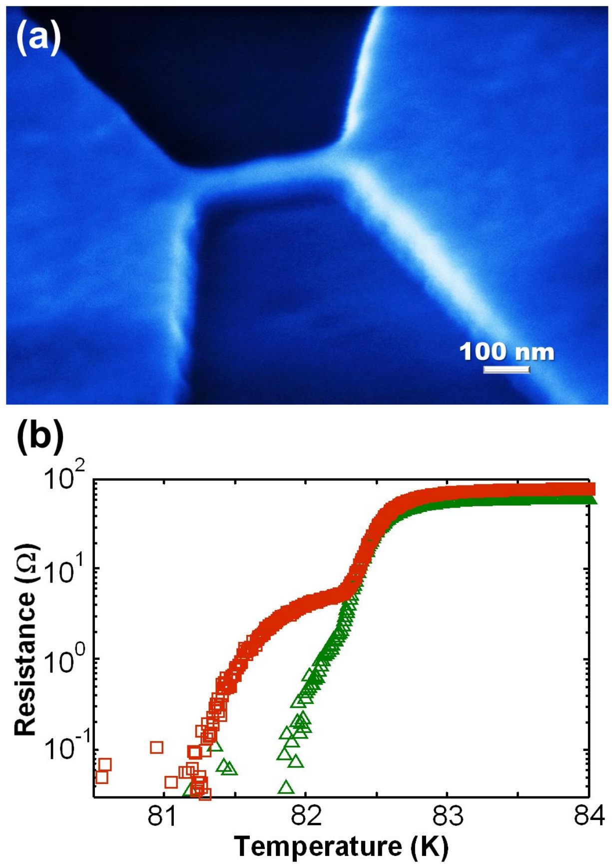

Figure 1: (a) Tilted angle scanning electron microscope (SEM) image of a 50 nm wide and 200 nm long Au capped YBCO nanowire grown on MgO (110). (b) $R(T)$ measurements of two nanowires grown on MgO (110), having a width of 50 nm (squares) and 150 nm (triangles). The length of both these wires is 200 nm.

published elsewhere [14, 15, 16]. The resistance of the YBCO nanowires with various widths has been measured as a function of the temperature, in a temperature range around T_C (see Fig. 1(b)). The current and voltage probes of our 4-point measurement setup are situated at the far ends of the two wide and long electrodes, with widths $w > 10^4$ nm and $l > 10^5$ nm, connected to the nanowires, whose length is 200 nm and width is in the range $50 - 150$ nm. We attribute the first transition in the $R(T)$ at higher temperatures to the electrodes and the second broader transition instead to the nanowires. Differently from what previously reported in literature [17], the onset temperature of the wire transition is typically only 1 K (or less) below the one of the wide electrodes, even for the narrowest wires.

It is important to note that the measured onset temperature of the wide electrodes, and consequently that of the wire, is 1-2 K lower than the expected one, corresponding to the value of the bare YBCO films. As already pointed out and discussed in detail in Ref. [18], this is only due to the additional resistive shunt of the Au film (which can be roughly approximated by the resistance R_{sh} of the gold strip of length $l_{Au} = l_{wire}$ and width $w_{Au} = w_{wire}$, on top of the YBCO wire) and not to a change of the superconducting transition temperature of the film.

The temperature broadening in the $R(T)$ of the wires (see Fig. 1(b)) can be analyzed according to the model previously discussed, thence considering vortices crossing the wires as the dominating source of resistance during the superconducting transition. According to this model, the resistive transition gets broader in temperature for decreasing wire width, in complete agreement with what we observe in our nanowires (see Fig. 1(b)). Indeed the barrier for vortex entry, expressed by eq. (1), depends explicitly on the wire width. Thence, we have ruled out models like the Berezinskii-Kosterlitz-Thouless (BKT) theory [19], related to vortex-antivortex pair dissociation in

2-dimensional systems with lateral extensions smaller than λ_P, which does not predict any size dependence in the $R(T)$ broadening.

In order to describe the broadening of the resistive transition in terms of vortex slips, we have considered the energy barrier for vortex entry expressed by eq. (1) [9]. As a consequence, the resistance of a YBCO wire is given by eq. (3). For the temperature dependence of the London penetration depth in the full temperature range we have used the two fluid model $\lambda_L(T) = \lambda_0 \left(1 - (T/T_C)^2\right)^{-1/2}$ [20]. An approximate expression for the temperature dependence of the coherence length can be obtained from the formula of the Ginzburg Landau depairing current density [21]

$$J_d = \frac{\Phi_0}{3\sqrt{3}\pi\mu_0\lambda_L^2(T)\xi(T)} \ , \tag{4}$$

and from the Bardeen expression for the temperature dependence of the depairing current density $J_d(T) \propto \left(1 - (T/T_C)^2\right)^{3/2}$ [22], characteristic of our nanowires [15] and of YBCO nanowires reported in literature [23], resulting in $\xi(T) = \xi_0 \left(1 - (T/T_C)^2\right)^{-1/2}$, which is valid in the full temperature range.

Since our wires are covered by a gold capping layer acting as a shunt, the final resistance can be expressed as:

$$R(T) = \left[R_v^{-1}(T) + R_{sh}^{-1}\right]^{-1} . \tag{5}$$

We have fitted the $R(T)$ of the wires, both grown on MgO (110) and MgO (001), with eq. (5), inserting the dimensions determined with AFM/SEM and extracting as fitting parameters the zero temperature values λ_0 and ξ_0, and the onset T_C of the critical temperature of the bare YBCO nanowires (see Fig. 2).

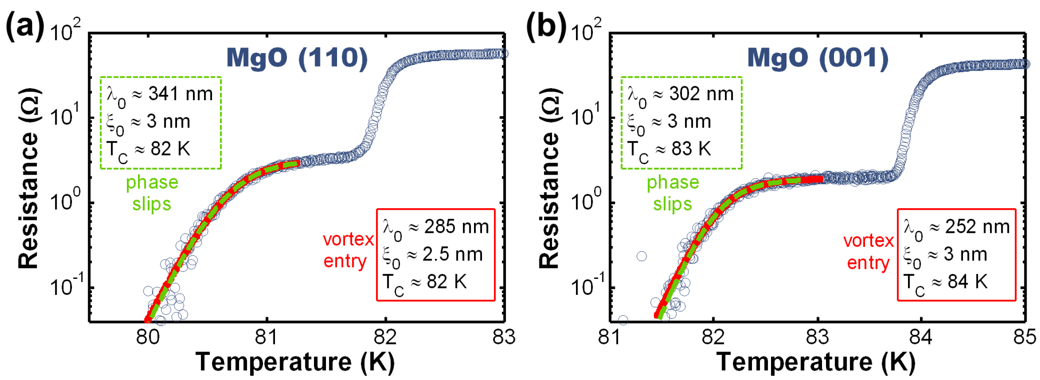

Figure 2: We have fitted with the vortex slip model (solid line) and with the Little model (dashed line) the R(T) curve of (a) a 85 nm wide wire grown on MgO (110); (b) a 67 nm wide wire grown on MgO (001).

A summary of the parameters extracted by the fits on different wires grown both on MgO (110) and MgO (001) is shown in Table 1.

Substrate	λ_0^v (nm)	ξ_0^v (nm)	J_d^v (A/cm^2)	λ_0^{ps} (nm)	ξ_0^{ps} (nm)	J_d^{ps} (A/cm^2)	J_c^{exp} (4.2 K) (A/cm^2)
MgO (110)	255-290	2-3	$\approx 5.5 \cdot 10^7$	325-350	2-3	$\approx 3.6 \cdot 10^7$	$\approx 6 - 9 \cdot 10^7$
MgO (001)	225-255	2-3	$\approx 7 \cdot 10^7$	300-325	2-3	$\approx 4 \cdot 10^7$	$\approx 8 - 10 \cdot 10^7$

Table 1: Summary of the parameters extracted from the fits of the $R(T)$ of nanowires with widths in the range $50 - 150$ nm, considering vortex slip (v) and phase slip (ps) models. The values of J_d^v and J_d^{ps} have been derived using eq. (4). The measured J_d^{exp} values have been taken from Ref. [15].

Since the height of the vortex entry barrier has been demonstrated to be similar to that of phase slips for sufficiently narrow nanowires ($w < 5\,\xi(T)$ at temperatures close to T_C, which is actually our case) [10], we have also fitted the $R(T)$ curves of our nanowires with the Little model, which is generally used to describe the non-zero resistance present below the transition temperature in terms of thermally activated phase slips [24], and compared the values of the extracted parameters with those of the vortex entry model (see Fig. 2). According to the Little model, the resistance of the nanowires can be written as in eq. (5), substituting the vortex entry resistance $R_v(T)$ with the Little resistance $R_{Little}(T)$:

$$R_{Little}(T) = R_N \exp\left(-\frac{\Delta F(T)}{k_B T}\right) . \tag{6}$$

Here, R_N is the normal resistance of the wire and $\Delta F(T)$ is the energy barrier for phase slip nucleation, which writes analytically as:

$$\Delta F(T) = \frac{4\epsilon_0(T)}{3\pi\sqrt{2}} \frac{w}{\xi(T)} . \tag{7}$$

A summary of the extracted parameters is shown in Table 1: in particular, the λ_0 values we obtain by fitting with the Little expression are more than 20% higher than those extracted from the vortex slip fit.

To obtain a confirmation on the validity of the used models, we have calculated the expected Ginzburg-Landau depairing current density J_d of the nanowires (eq. 4) using the values of ξ_0 and λ_0 extracted from both the fits, which are typical of YBCO thin films [25, 26]. In particular if one is considering vortex slips as the main source of resistance, the expected values of the critical current density, J_d^v, are rather consistent with the J_c^{exp} we have extracted from the IV curves at 4.2 K [15, 18]. Moreover, comparing nanowires grown on MgO (110) and MgO (001), the difference between the extracted J_d is consistent both with the difference between the measured J_C at 4.2 K [15] and with the lower T_C measured on films grown on MgO (110), as a consequence of the large mismatch between the film/substrate in-plane lattice parameters. On the contrary, the discrepancy with the measured J_c^{exp} values significatively increases when calculating the expected Ginzburg-Landau depairing current density J_d of the nanowires with the ξ_0 and λ_0 values extracted from the Little fit (see Table 1).

As a further proof of the validity of the parameters extracted by using the thermally activated vortex entry model, we also extracted the London penetration depth from the critical current modulations of a YBCO nanoSQUID patterned on a MgO (110) substrate as a function of an externally applied magnetic field [27]. Our devices, made by two parallel nanowires connecting two wider electrodes (Dayem bridge configuration) (see Fig. 3(a)), are characterized by a modulation of the critical current as a function of an external magnetic field in the whole temperature range from 300 mK up to their critical temperature (see Fig. 3(b)). By numerically calculating the magnetic field pattern of the critical current of a nanoSQUID using the Likharev-Yakobson expression for the current phase relation of a long nanowire [28, 29, 30], $I(\phi) = \Phi_0 wt\left[(\xi/l)\phi - (\xi/l)^3\phi^3\right]/2\pi\mu_0\xi\lambda_L^2$, we obtain that, from the critical current modulation depth $\gamma = \Delta I_C/I_C^{max}$, the screening inductance factor β_L of the devices can be determined for each temperature as $1/\gamma$ (see Fig. 3(c)). The parameter $\beta_L(T)$, defined as $I_C^{max}(T)L_{loop}(T)/\Phi_0$, with L_{loop} total inductance of the SQUID loop and Φ_0 flux quantum, can be numerically calculated by solving the Maxwell and London equations describing the Meissner state on our SQUID geometry [31]. For the temperature dependence of the loop inductance we have again used the two fluid model for the London penetration depth, on which the kinetic inductance of the wires (which gives the main contribution to L_{loop}) is strongly dependent. Thence,

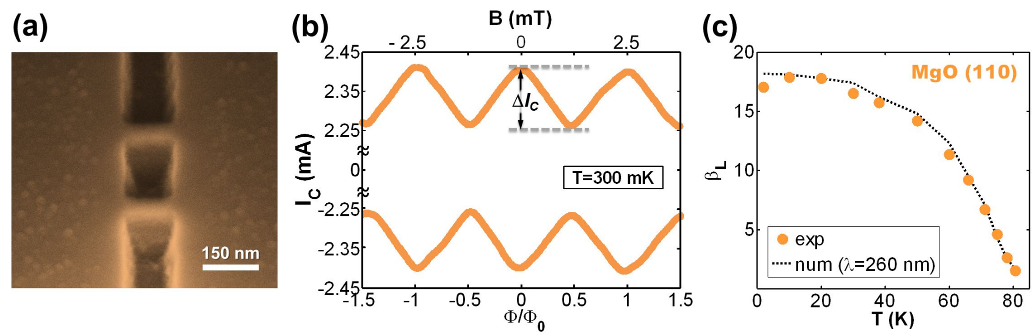

Figure 3: (a) SEM picture of a Dayem bridge nanoSQUID, patterned on MgO(110), with a loop area of 130×150 nm^2. (b) Critical current of the same device measured at 300 mK as a function of the applied magnetic field. (c) From the critical current modulation depth $\Delta I_C/I_C^{max}$ we have estimated for each temperature the screening inductance factor β_L. This experimentally determined parameter can be fitted with a numerically calculated screening inductance factor, using λ_0 as the only fitting parameter. The agreement between data and numerical calculation is very good using $\lambda_0 = 260$ nm, in accordance with the value extracted by the vortex entry fit of the $R(T)$ of YBCO nanowires grown on MgO (110).

the experimentally determined β_L can be fitted with the numerically calculated one, using λ_0 as the only fitting parameter. As shown in Fig. 3(c), the agreement between data and numerical computations is very good using $\lambda_0 = 260$ nm. Such a value is in the range, shown in Table 1, of the λ_0 values we can extract, by using the vortex entry model, from the $R(T)$ of the YBCO nanowires grown on MgO (110) substrates.

All these results give a confirmation of the validity of the vortex slip fitting procedure to extract physical quantities, as ξ_0 and λ_0, representing the nanowire. The possibility to explain the broadening in the resistive transition only in terms of the dissipation due to vortices crossing the wire proves the high quality of our nanostructures, preserving pristine superconducting properties because of the presence of the gold capping layer. Moreover, the magnetic field response of the critical current observed in our nanowire based nanoSQUIDs in the full temperature range below T_C makes them very attractive as magnetic flux detectors in the field of nano-magnetism [32].

Acknowledgement

This work has been partially supported by the Swedish Research Council (VR) and the Knut and Alice Wallenberg Foundation. R.A. was partially supported by a grant from the Foundation BLANCEFLOR Boncompagni Ludovisi, née Bildt. M.A. acknowledges support from the Marie Curie Initial Training Action (ITN) Q-NET 264034. G.K. has been supported by the Svenska Institute under the project "Complex oxide films at the nanoscale".

References

[1] P. Ao, D. J. Thouless, Phys. Rev. Lett. 72 (1994) 132–135.

[2] F. Tafuri, J. R. Kirtley, D. Born, D. Stornaiuolo, P. G. Medaglia, P. Orgiani, G. Balestrino, V. G. Kogan, EPL (Europhysics Letters) 73 (2006) 948.

[3] A. Engel, A. Semenov, H.-W. Hubers, K. Ilin, M. Siegel, Physica C: Superconductivity 444 (2006) 12 – 18.

[4] W. A. Little, Phys. Rev. 156 (1967) 396–403.

[5] J. S. Langer, V. Ambegaokar, Phys. Rev. 164 (1967) 498–510.

[6] D. E. McCumber, B. I. Halperin, Phys. Rev. B 1 (1970) 1054–1070.

[7] C. Qiu, T. Qian, Phys. Rev. B 77 (2008) 174517.

[8] H. Bartolf, A. Engel, A. Schilling, K. Il'in, M. Siegel, H.-W. Hübers, A. Semenov, Phys. Rev. B 81 (2010) 024502.

[9] L. N. Bulaevskii, M. J. Graf, C. D. Batista, V. G. Kogan, Phys. Rev. B 83 (2011) 144526.

[10] D. Y. Vodolazov, Phys. Rev. B 85 (2012) 174507.

[11] A. Gurevich, V. M. Vinokur, Phys. Rev. B 86 (2012) 026501.

[12] L. G. Aslamazov, S. V. Lempitsky, Zh. Eksp. Teor. Fiz. 84 (1983) 2216.

[13] D. Y. Vodolazov, I. L. Maksimov, E. H. Brandt, EPL (Europhysics Letters) 48 (1999) 313.

[14] S. Nawaz, R. Arpaia, F. Lombardi, T. Bauch, Phys. Rev. Lett. 110 (2013) 167004.

[15] S. Nawaz, R. Arpaia, T. Bauch, F. Lombardi, Physica C 495 (2013) 33 – 38.

[16] R. Arpaia, M. Ejrnaes, L. Parlato, R. Cristiano, M. Arzeo, T. Bauch, S. Nawaz, F. Tafuri, G. P. Pepe, F. Lombardi, Supercond. Sci. Technol. 27 (2014) 044027.

[17] G. Papari, F. Carillo, D. Stornaiuolo, L. Longobardi, F. Beltram, F. Tafuri, Supercond. Sci. Technol. 25 (2012) 035011–035015.

[18] R. Arpaia, S. Nawaz, F. Lombardi, T. Bauch, IEEE Trans. Appl. Supercond. 23 (2013) 1101505.

[19] M. R. Beasley, J. E. Mooij, T. P. Orlando, Phys. Rev. Lett. 42 (1979) 1165–1168.

[20] M. Tinkham, Introduction to Superconductivity, Dover Publications, 2004.

[21] J. R. Clem, V. G. Kogan, Phys. Rev. B 86 (2012) 174521.

[22] J. Bardeen, Rev. Mod. Phys. 34 (1962) 667–681.

[23] Z. G. Ivanov, N. Y. Fogel, O. I. Yuzephovich, E. A. Stepantsov, A. Y. Tzalenchuk, Low Temperature Physics 30 (2004) 203.

[24] A. Bezryadin, J. Phys.: Condens. Matter 20 (2008) 043202.

[25] A. G. Zaitsev, R. Schneider, G. Linker, F. Ratzel, R. Smithey, P. Schweiss, J. Geerk, R. Schwab, R. Heidinger, Rev. Sci. Instrum. 73 (2002) 335–344.

[26] N. Belk, D. E. Oates, D. A. Feld, G. Dresselhaus, M. S. Dresselhaus, Phys. Rev. B 53 (1996) 3459–3470.

[27] R. Arpaia, M. Arzeo, S. Nawaz, S. Charpentier, F. Lombardi, T. Bauch, Appl. Phys. Lett. 104 (2014) 072603.

[28] K. K. Likharev, L. A. Yakobson, Sov. Phys. Tech. Phys. 20 (1976) 950.

[29] K. Likharev, Reviews of Modern Physics 51 (1979) 101.

[30] M. Y. Kupriyanov, K. K. Likharev, Fiz. Tverd. Tela 16 (1974) 2829.

[31] J. Johansson, K. Cedergren, T. Bauch, F. Lombardi, Phys. Rev. B 79 (2009) 214513.

[32] C. Granata, A. Vettoliere, R. Russo, M. Fretto, N. De Leo, V. Lacquaniti, Appl. Phys. Lett. 103 (2013) 102602.